

## Temperature Relaxation in Hot Dense Hydrogen

Michael S. Murillo<sup>1,\*</sup> and M. W. C. Dharma-wardana<sup>2,†</sup>

<sup>1</sup>*Physics Division, Los Alamos National Laboratory, Los Alamos, New Mexico 87545, USA*

<sup>2</sup>*National Research Council, Ottawa, Canada K1A 0R6*

(Received 7 December 2007; published 23 May 2008)

Temperature equilibration of hydrogen is studied for conditions relevant to inertial confinement fusion. New molecular-dynamics simulations and results from quantum many-body theory are compared with Landau-Spitzer predictions for temperatures  $T$  with  $50 < T < 4000$  eV and densities with Wigner-Seitz radii  $r_s = 1.0$  and  $0.5$ . The relaxation is slower than the Landau-Spitzer result, even for  $T$  in the kilo-electron-volt range, but converge to agreement in the high- $T$  limit.

DOI: 10.1103/PhysRevLett.100.205005

PACS numbers: 52.25.Kn, 52.27.Gr, 71.10.-w

*Introduction.*—While a first-principles description of the equilibrium properties of strongly coupled Coulomb systems is a formidable task [1], nonequilibrium systems pose an even greater challenge. Short-pulse lasers and shock waves create nonequilibrium states; thus, Coulomb systems as diverse as warm dense matter [2], ultracold plasmas [3], shocked semiconductors [4], and dense deuterium [5] can now be created, but initially under nonequilibrium conditions. Similarly, energy relaxation (ER) in astrophysical plasmas is important to the physics of fusion of various elements in determining stellar evolution [6]. Here, we consider the ER of nonequilibrium dense hydrogen important in inertial confinement fusion (ICF) [7]. The theory of these dense plasmas covers physical processes over many orders of magnitude in both density and temperature.

The earliest theories of ER in plasmas were formulated by Landau [8] and Spitzer [9] (denoted LS). LS is applicable to dilute, hot, fully ionized plasmas where the collisions are weak and binary. Essentially, LS is Rutherford's Coulomb scattering formula applied to Maxwellian distributions. A characteristic feature of the LS approach is the use of a Coulomb logarithm, i.e.,

$$\mathcal{L} = \ln \Lambda = \int_{b_{\min}}^{b_{\max}} db/b \sim \int_{k_{\min}}^{k_{\max}} dk/k, \quad (1)$$

where  $b_{\min}$  (or  $1/k_{\max}$ ) and  $b_{\max}$  (or  $1/k_{\min}$ ) are suitable, but *ad hoc* impact parameter (or momentum) cutoffs for the Coulomb collision. Convergent kinetic equations [10,11] have been developed to resolve the divergences that require the cutoffs. The full quantum approach, based on calculating a transition rate, however, does not suffer from the need for cutoffs. Calculations at the Fermi golden-rule (FGR) level and beyond have been made by Dharma-wardana *et al.* [12–14]. Such methods automatically include degeneracy effects, collective modes, and strong coupling. Hansen and McDonald (HM) [15] and Reimann and Toepffer [16] have directly obtained ER rates via molecular-dynamics (MD) simulations. HM concluded that many-body effects are negligible and that the LS result holds [15]. In contrast, compared to LS, theoretical approaches that use the time development of the one-body

distribution relax faster [11], while those using the dynamic structure factor relax more slowly [12,14].

There is currently no direct experimental data for ER rates, although such experiments are underway [17,18]. Here, we present larger HM-like MD simulations and quantum many-body calculations to narrow the gap in predicted ER rates for hot, dense hydrogen relevant to ICF targets composed of dense cryogenic fuel rapidly laser compressed to kilo-electron-volt temperatures. In a hydrogen plasma the particle charges  $z_i, z_j$  are  $\pm 1$ , in atomic units, where the electronic charge  $|e| = \hbar = m_e = 1$ . The mean electron and proton densities  $n$  and  $\rho$  are identical. The ratio of a typical Coulomb energy to the kinetic energy becomes, in the classical regime,  $\Gamma = 1/(r_s T)$ , and simply  $r_s$  in the quantum regime. Here  $T$  is the temperature in energy units and  $r_s = [3/(4\pi n)]^{1/3}$  is the Wigner-Seitz radius. The properties of partially degenerate, fully ionized plasmas require two independent parameters, e.g., both  $r_s$  and  $\theta = T/E_F$ , where  $E_F = \frac{1}{2}(3\pi^2 n)^{2/3}$  is the Fermi energy [19].

*Molecular dynamics.*—Nonequilibrium quantum simulations require theoretical breakthroughs that are not yet fully established. However, MD techniques that employ quantum-corrected effective potentials can be used for these problems. Since MD simulations attempt to solve the many-body equations of motion exactly, they are likely to provide accurate ER rates for hot, dense hydrogen. Several issues arise in simulations with  $T$  in the  $10^2$ – $10^3$  eV range, however, because the screening length and mean-free-path are larger at higher  $T$ ; thus, we have varied the number of particles widely (maximum of several thousand), with  $N = 500$  used for the results presented here. This is about 4 times that used by HM. Also, because the ER time varies roughly as  $T_e^{3/2}$ , these simulations required  $>10^6$  time steps for the higher- $T$  cases. Compounding the longer runs was the need for much smaller time steps (as small as  $0.005\omega_{pe}^{-1}$ , where  $\omega_{pe}$  is the electron plasma frequency). This is a result of high velocity collisions important at high  $T$ . Such issues are not unexpected, but have rarely been dealt with, since MD is typically applied to strongly coupled (i.e., cooler) classical

systems. We carried out direct simulations of electrons and protons since the Born-Oppenheimer approximation is not applicable to this problem. The mass ratio 1:1836 was used because of our interest in mass-dependent collective mode effects. Finally, integrations were carried out with the velocity-Verlet algorithm using an  $\mathcal{O}(N^{3/2})$  Ewald method.

The classical Coulomb interaction  $1/r$  is replaced by the mean value of the operator  $1/\hat{r}$  in quantum systems. This feature modifies the short-range behavior of the electron-electron and electron-proton interactions, since the de Broglie wavelength of the electron is not negligible for small  $r$ . Also, unlike the classical electron-proton interaction which always leads to a bound state, the delocalized electron does not bind to the proton for regimes studied here. These effects are included in the  $e-e$  and  $e-p$  potentials by solving the relevant Schrödinger equations for the two-body scattering processes. These lead to diffraction-corrected Coulomb potentials  $v_{ij}^{\text{dfr}}(r_{ij})$  which are Coulomb-like for distances larger than the respective de Broglie lengths,  $\lambda_{ij} = 1/\sqrt{2\pi\mu_{ij}T_e}$ . Here  $\mu_{ij}$  are the effective masses of the colliding pair. The choice of  $b_{\text{min}} = \lambda_{ij}$  is common in the LS approaches.

The interaction  $\phi_{ij}(r)$  between the pair  $i, j$  is given by

$$\phi_{ij} = v_{ij}^{\text{dfr}}(r_{ij}) + v_{ee}^{\text{Pau}}(r_{ij}) \quad (2)$$

$$v_{ij}^{\text{dfr}}(r_{ij}) = \frac{z_i z_j}{r_{ij}} [1 - e^{-(f_{ij} r_{ij})/\lambda_{ij}}] + v_{ij}^{\text{Ewl}}(r_{ij}), \quad (3)$$

where  $v_{ij}^{\text{Ewl}}$  is the Ewald potential. The potential  $v_{ee}^{\text{Pau}}$  accounts for the spin-averaged Pauli exclusion between two electrons. This ensures that the “noninteracting” electron pair distribution functions (PDFs) calculated from a classical simulation are exactly the noninteracting quantum PDFs [20,21]. The explicit form [22] used by HM is adequate for most of the range studied in this Letter. The factor  $f_{ij}$  is unity for all except the cross-species case  $f_{ep}$ , which is chosen using the classical-map-hypernetted-chain (CHNC) method. CHNC uses the above  $v_{ij}$  and a classical fluid temperature  $T_{cf} = \sqrt{T_e^2 + T_q^2}$ , where the quantum temperature  $T_q$  is defined in Ref. [21]. The factor  $f_{ep}$  at a given  $r_s$ ,  $T_e$ , and  $T_p$  is fixed by requiring that the CHNC  $g_{ep}(r)$ , at  $r = 0$ , is the same as the Kohn-Sham value of  $g_{ep}(r = 0)$ , as discussed more fully in Ref. [23]. We found that the  $f_{ep}$  are within 5% of unity for the conditions of our study. The use of a  $T_{cf}$  in CHNC, and a  $T_e$  in the classical MD, lead to no inconsistency in the regime of interest, as shown in Fig. 1 where setting  $T_q = 0$  is shown to have no perceptible effect. The potentials are validated under quasiequilibrium ( $T_e \neq T_i$ ) dense-plasma conditions, via CHNC and MD (using  $\phi_{ij}$  and its simplified HM forms) for  $r_s = 1.0$ ,  $T_e = 50$  eV, and  $T_i = 10$  eV. In the MD, electron and proton velocity-scaling thermostats were used to create the two-temperature system, whereas recent results for the cross-species temperature  $T_{ep}$  [23] were used in the CHNC. The PDFs  $g_{ij}(r)$  are shown in Fig. 1.

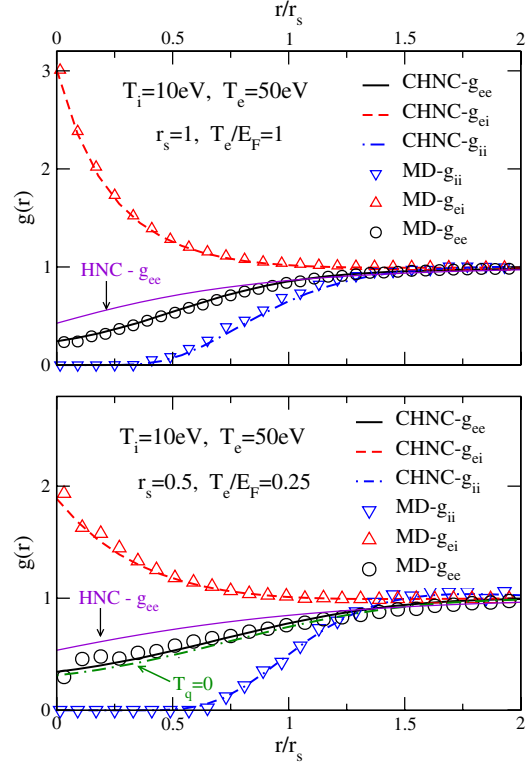


FIG. 1 (color online). Pair distribution functions from MD (data points), CHNC (thick lines) for dense hydrogen,  $r_s = 0.5$  and  $1$ ,  $T/E_F = 0.25$  and  $1$ . The  $g_{ee}$  from a simple HNC calculation (i.e., no  $T_q$ , no Pauli potential) with only  $v_{ij}^{\text{dfr}}$  is also shown. The bottom panel shows a CHNC  $g_{ee}$  with  $T_q = 0$ , showing that  $T_q$  is of no significance in the regime of interest.

ER rates were determined for the two densities  $r_s = 0.5$  ( $n_e = 1.3 \times 10^{25} \text{ cm}^{-3}$ ) and  $r_s = 1.0$  ( $n_e = 1.61 \times 10^{24} \text{ cm}^{-3}$ ) over the temperature range  $0.25 < \theta < 20$ . In practice, an equilibration stage with separate electron and proton velocity-scaling thermostats was used to establish a two-temperature system. This was followed by a micro-canonical evolution in which the temperatures were relaxed, with

$$T_j(t) = \frac{m_j}{3N_j} \sum_{i=1}^{N_j} v_j^2(t), \quad (4)$$

for each species  $j$ . Energy conservation was monitored to assure stability at elevated  $T$ . Stability was quantified by  $\Delta E = \frac{1}{N} \sum_{i=1}^N | \frac{E_i - E_0}{E_0} |$ , where  $E_i$  is the energy at the  $i$ th time step. The time step was chosen via several simulations with varying time steps for  $T_e = 100, 250, 500,$  and  $750$  eV and noting the impact on  $\Delta E$ . As noted above, the time step required for stability decreases dramatically with increasing  $T$ . A fit to the slope of the temperature profiles yielded the equilibration rate; in practice, the ion temperature was fixed for all runs at  $T_i = 10$  eV so that the reported results are  $\partial T_e / \partial t$ . For the  $T_e, T_i$  considered, ER is insensitive to the value of  $T_i$  itself.

*Quantum transition rates.*—The most transparent, strictly quantum approach to the calculation of the ER rate is to treat it as a transition rate where an electron in an initial momentum state  $\vec{k}_i$  transfers to a final state  $\vec{k}_f$ , while a proton in the initial momentum eigenstate  $\vec{p}_i$  absorbs energy and transfers to a final eigenstate  $\vec{p}_f$ . The availability of such states depends on the products of Fermi occupation factors  $n_{k_i}(1 - n_{k_f})$ , and similarly for the proton states. The strength of the transition depends on the matrix element between the initial and final states. This matrix element may be taken in lowest-order theory (Born approximation) or in higher order (i.e., a  $T$ -matrix evaluation). These are the usual ingredients of the FGR for the transition rate. The summation over all such pair processes gives the total ER rate. But such summations immediately convert the description of the plasma into a description in terms of its excitation modes. The spectrum of all modes is given by the spectral function  $A_j(q, \omega, T_j)$  where the species index  $j = e$  or  $p$ . These spectral functions are given by the imaginary parts of the corresponding dynamic response functions  $\chi^j(\vec{k}, \omega)$ , e.g., Eq. (16) of Ref. [14]. The ER rate evaluated within the FGR,  $R_{\text{FGR}}$ , can be expressed in terms of the response functions of the plasma as follows, given in Eqs. (4)–(7) of Refs. [13] and Ref. [14]:

$$R_{\text{FGR}} = \frac{dK}{dt} = \int \frac{d^3k}{(2\pi)^3} \frac{\omega d\omega}{2\pi} (\Delta B) F_{ep} \quad (5)$$

$$\Delta B = \coth(\omega/2T_e) - \coth(\omega/2T_p) \quad (6)$$

$$F_{ep} = |(V_{ep}(k)|^2 \text{Im}[\chi^p(k, \omega)] \text{Im}[\chi^e(k, \omega)] \quad (7)$$

In the above we have used the spherical symmetry of the plasma to write scalars  $q, k$  instead of  $\vec{q}, \vec{k}$ , to simplify the notation. Other discussions of dynamic structure factors have been given by Boercker and More [24].

The excess-energy density is denoted by  $K = K_e - K_i$ , and becomes  $3(T_e - T_p)n/2$  only in the classical regime, i.e., where the chemical potential  $\mu$  is negative. The interaction  $V_{ep}(k)$  in this equation is the full Coulomb matrix element and *not* the diffraction-corrected form used in the CHNC and classical simulations. In the simplest form of the FGR,  $V_{ep}(k) = 4\pi/k^2$  since the momentum states are taken to be plane waves. A  $T$ -matrix evaluation would use phase-shifted plane waves and the corresponding modified density of states, instead of  $d^3k/(2\pi)^3$ . With the onset of the classical regime where  $\mu < 0$ , which occurs for  $\theta > 1$ , the  $\Delta B$  factor becomes  $2\Delta/\omega$  where  $\Delta = (T_e - T_p)$ . It was shown in Hazak *et al.* [14] how to perform the  $\omega$  integration by exploiting the  $f$ -sum rule and the fact that the ion-spectral function, peaking near the ion-plasma frequency, resides far below the electron spectral function. Then Eq. (5) can be written, to a good approximation, as

$$\frac{1}{\Delta} \frac{d\Delta}{dt} = \frac{2}{3n} \omega_{\text{ion}}^2 \int_0^\infty \frac{2}{\pi} \left[ \frac{\partial}{\partial \omega} \text{Im} \chi^{ee}(k, \omega) \right]_{\omega=0} dk, \quad (8)$$

where  $\omega_{\text{ion}}$  is the proton-plasma frequency. If we keep the proton temperature  $T_p$  fixed, we see that Eq. (8) leads to a relaxation time  $\tau$  for the electron temperature  $T_e$ , involving the inverse of the right-hand side of Eq. (8).

The above analysis treats the plasma as two independent subsystems. In reality, the ion-density fluctuations are screened by the electron subsystem, and the ion-plasma excitation becomes an ion-acoustic mode. The excitations in the coupled-mode (CM) system are described by the zeros of Eq. (45) of Ref. [12]. In the static  $k \rightarrow 0$  limit this denominator converts the electron screening parameter  $k_{DH}^e$  to  $\sqrt{\{(k_{DH}^e)^2 + (k_{DH}^p)^2\}}$ . However, the proton-density fluctuations act dynamically in the relaxation process, and the use of static ion screening is incorrect. The CM approach is fully dynamical and includes another denominator, viz.,

$$d_{\text{CM}} = |1 - V_{ep}^2(k) \chi^{ee}(k, \omega) \chi^{pp}(k, \omega)|^2, \quad (9)$$

in the integrand in Eq. (5). That is,  $F_{ep}$  in Eq. (5) is replaced by  $F_{ep}/d_{\text{CM}}$ .

The simple LS form can also be written in the same form as Eq. (8), as shown in Ref. [14]. The quantum approaches

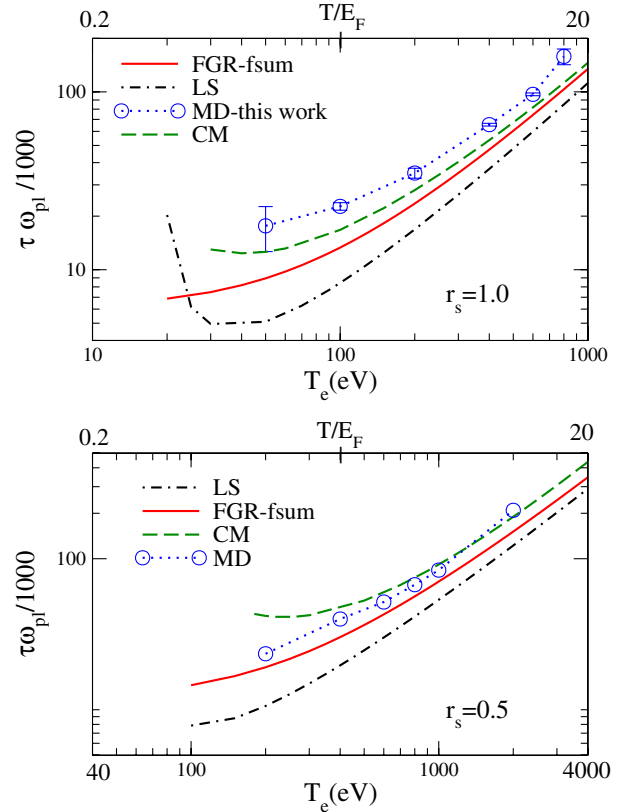


FIG. 2 (color online). The relaxation time  $\tau/1000$ , in units of the inverse electron-plasma frequency, for dense hydrogen,  $r_s = 0.5$  and  $1$ , from the degenerate to the classical region. The Landau-Spitzer (LS) result [using the Hansen-McDonald (HM) prescription for the  $k$  cutoffs], the results from the Fermi golden rule (FGR), and the coupled-mode (CM) are shown together with the MD results.

in CM and FGR automatically and self-consistently contain diffraction and screening contributions. Thus, while Eq. (8) uses the full integration  $k = 0 \rightarrow \infty$ , LS needs the cutoffs  $k_{\min}$  and  $k_{\max}$  to obtain a convergent result, and the calculated LS values of  $\tau$  are therefore dependent on the particular choice of  $k_{\min}$  and  $k_{\max}$ . Hence, different realizations of the LS form need not yield the same result. For example, Lee and More [25] use cutoffs based on the full static screening length, including the ions; however, the CM analysis clearly shows that the ion response in ER is dynamic.

The noninteracting response function  $\chi^0(q, \omega, T)$  at arbitrary degeneracies was given by Khanna and Glyde [26]. We use a form where local field corrections  $G_{ee}(k)$  may be included [12], but such corrections are quite small under ICF conditions. Both the FGR and CM assume linear response for the interaction of a proton with the electrons. The resulting calculations are shown in Fig. 2. The CM calculation is quite close to the FGR  $f$ -sum result. This is expected since the H plasmas considered here are relatively weakly coupled, with  $\Gamma \sim 1$  or less. Nevertheless, the inclusion of CM leads to better agreement with the MD simulation. Also, we have assumed the bare  $4\pi/k^2$  form for the  $V_{ep}$  in the FGR and CM formulas, without the moderating effects of a pseudopotential. Such effects would tend to make  $\tau$  larger than that from the present FGR or CM calculation. The linear-response assumption is more satisfactory for the  $r_s = 0.5$  plasma. Thus the MD results at  $r_s = 0.5$  are very close to the CM results.

*Conclusion.*—We have evaluated the temperature relaxation time in hot, dense hydrogen using both state-of-the-art molecular-dynamics simulations and quantum many-body theory. The FGR provides a convenient estimate which needs a small correction from the dynamical coupled-mode effects. The good agreement between simulation and theory is very encouraging, and suggests that linear-response assumptions may be the source of existing differences. We find that the relaxation is slower than the LS value even for temperatures in the kilo-electron-volt range, which suggests that burning plasmas are slightly more out of equilibrium than might have been expected. In contrast to the calculations presented in, say, Refs. [12,13], where strongly coupled Al plasmas were considered, the present calculations are for hydrogenic systems with  $\Gamma \sim 1$  or less, and the temperatures have been pushed to  $T/E_F \simeq 20$ . Thus, we see that the CM, FGR, and the LS forms converge for sufficiently large  $T/E_F$ . It is clear that the LS form is inadequate for highly compressed, moderate- $T$ , partially degenerate plasmas, in agreement with the main message of Ref. [12].

---

\*murillo@lanl.gov

†chandre@argos.phy.nrc.ca

- [1] P. Umari, A. J. Williamson, G. Galli, and N. Marzari, *Phys. Rev. Lett.* **95**, 207602 (2005); C. Pierleoni, D. M. Ceperley, and M. Holzmann, *Phys. Rev. Lett.* **93**, 146402 (2004); C. Dharma-wardana and F. Perrot, *Phys. Rev. B* **66**, 014110 (2002).
- [2] D. Riley, N. C. Woolsey, D. McSherry, I. Weaver, A. Djaoui, and E. Nardi, *Phys. Rev. Lett.* **84**, 1704 (2000).
- [3] Y. C. Chen, C. E. Simien, S. Laha, P. Gupta, Y. N. Martinez, P. G. Mickelson, S. B. Nagel, and T. C. Killian, *Phys. Rev. Lett.* **93**, 265003 (2004).
- [4] P. Celliers, A. Ng, G. Xu, and A. Forsman, *Phys. Rev. Lett.* **68**, 2305 (1992).
- [5] M. D. Knudson, D. L. Hanson, J. E. Bailey, C. A. Hall, and J. R. Asay, *Phys. Rev. Lett.* **90**, 035505 (2003).
- [6] A. I. Chugunov, H. E. DeWitt, and D. G. Yakovlev, *Phys. Rev. D* **76**, 025028 (2007); F. A. Agronyan and R. A. Syunyaev, *Astrofiz.* **27**, 131 (1987) [*Astrophysics (Engl. Transl.)* **27**, 413 (1988)].
- [7] R. Linford, R. Betti, J. Dahlburg, J. Asay, M. Campbell, Ph. Colella, J. Freidberg, J. Goodman, D. Hammer, J. Hoagland, S. Jardin, J. Lindl, G. Logan, K. Matzen, G. Navratil, A. Nobile, J. Sethian, J. Sheffield, M. Tillack, and J. Weisheit, *J. Fusion Energy* **22**, 93 (2003).
- [8] L. D. Landau, *JETP* **7**, 203 (1937); E. M. Lifshitz and L. P. Pitaevskii, *Physical Kinetics* (Pergamon, Oxford, 1981).
- [9] L. Spitzer, *Physics of Fully Ionized Gases* (Interscience, New York, 1967).
- [10] H. A. Gould and H. E. DeWitt, *Phys. Rev.* **155**, 68 (1967).
- [11] D. O. Gericke, M. S. Murillo, and M. Schlanges, *Phys. Rev. E* **65**, 036418 (2002).
- [12] M. W. C. Dharma-wardana and F. Perrot, *Phys. Rev. E* **58**, 3705 (1998); **63**, 069901 (2001).
- [13] M. W. C. Dharma-wardana, *Phys. Rev. E* **64**, 035401 (2001).
- [14] G. Hazak, Z. Zinamon, Y. Rosenfeld, and M. W. C. Dharma-wardana, *Phys. Rev. E* **64**, 066411 (2001).
- [15] J. P. Hansen and I. R. McDonald, *Phys. Lett. A* **97**, 42 (1983).
- [16] U. Reimann and C. Toepffer, *Laser Part. Beams* **8**, 771 (1990).
- [17] J. M. Taccetti *et al.*, *J. Phys. A* **39**, 4347 (2006).
- [18] J. J. Angulo Garetá and D. Riley, *High Energy Density Phys.* **2**, 83 (2006).
- [19] M. S. Murillo, *Phys. Plasmas* **11**, 2964 (2004).
- [20] F. Lado, *J. Chem. Phys.* **47**, 5369 (1967).
- [21] M. W. C. Dharma-wardana and F. Perrot, *Phys. Rev. Lett.* **84**, 959 (2000).
- [22] C. S. Jones and M. S. Murillo, *High Energy Density Phys.* **3**, 379 (2007).
- [23] M. W. C. Dharma-wardana and M. S. Murillo, *Phys. Rev. E* **77**, 026401 (2008).
- [24] D. B. Boercker and R. M. More, *Phys. Rev. A* **33**, 1859 (1986).
- [25] Y. T. Lee and R. M. More, *Phys. Fluids* **27**, 1273 (1984).
- [26] F. C. Khanna and H. R. Glyde, *Can. J. Phys.* **54**, 648 (1976).